
Heart Disease Recognition from heart beat audio signals

Ligari D. • Alberti A.¹

¹ *Department of Computer Engineering, Data Science, University of Pavia, Italy*
Course of Advanced Biomedical Machine Learning

Github page: <https://github.com/DavideLigari01/advanced-biomedical-project>

Date: July 2, 2024

Abstract — The early detection of heart diseases is crucial for reducing mortality, yet traditional diagnostic methods often fail to identify conditions until advanced stages. Leveraging advancements in machine learning, this study presents two different models aimed at enhancing heart disease detection from heart sound recordings. The models, MLP_Ensemble5 and MLP_Ensemble2, were developed using advanced ensemble techniques and optimized to balance computational efficiency with diagnostic accuracy. MLP_Ensemble5 focuses on minimizing false normals, and MLP_Ensemble2 emphasizes overall performance and incorporates explainability measures to aid medical professionals. The study utilizes a dataset of heart sound recordings, processed through steps of data preprocessing, feature extraction using several spectral coefficients (MFCCs, Chroma STFT...), and feature selection to develop robust predictive models. Despite promising results, the research faced limitations such as the small dataset size, leading to potential biases due to lack of a validation set, and challenges in capturing complete cardiac cycles with the chosen extraction intervals. Moreover, the models' explainability, necessitates further validation. Future work will focus on expanding the dataset, optimizing extraction intervals to capture full cardiac cycles, exploring alternative feature extraction techniques, and enhancing model explainability to ensure clinical applicability. This study demonstrates the potential of machine learning models in heart disease detection and underscores the need for further research to overcome current limitations and enhance model reliability in clinical settings.

Keywords — Heartbeat Classification • Machine Learning • Audio Features • Correlation Analysis • Ensemble Models

CONTENTS

1	Introduction	1
2	Methods	2
2.1	Source of Data	2
2.2	Data Preprocessing	4
2.3	Feature Extraction	5
2.4	Feature Selection	7
2.5	Models	8
2.5.1	Experimented Architectures	10
2.6	Tools and Software	10
3	Results	10
3.1	Prevention Model	10
3.2	Support Model	11
3.3	Other Experiments	14
4	Discussion	14
5	Conclusion	15
5.1	Future Works	15
6	Appendix	16

1. INTRODUCTION

Hear diseases are the leading cause of death world-wide, accounting for 18.5 million deaths in 2019, as reported by Max Roser in World In Data 2021 [11]. This highlights the urgent need for early detection to prevent fatalities. Traditional diagnostic methods often fall short, diagnosing heart conditions at advanced stages when treatment options are limited. Therefore, developing an automated system for early detection is crucial. Recent advancements in machine learning and deep learning have shown promise in healthcare applications, including heart disease detection. These technologies can offer accurate and early diagnosis, potentially improving patient outcomes. However, current models have limitations. For instance, simple models like SVM, used by Zhang et al. [12] and Deng et al. [6], have low precision, unsuitable for medical applications. Moreover, researches by Alafif et al. [2], Noman et al. [9] and Rath et al [Rath_Mishra_Panda_Pal_2022], focuses on identifying whether a heartbeat is normal or abnormal without specifying the type of disease. Additionally, Chen et al.'s [4] model, despite its high accuracy of 0.93, is too complex for practical usage and distinguishes only a few types of heart diseases, which is inadequate for comprehensive medical

applications.

To address these limitations, we propose a model that effectively identifies various heart diseases, including cases where no heart disease is present, while balancing model complexity with result accuracy.

Considering the importance of early anomaly detection in heartbeats, we also propose a lightweight model capable of detecting anomalies in heartbeat recordings. This approach allows individuals to use their smartphones to record their heartbeats and check for anomalies, facilitating timely consultation with a doctor for further diagnosis.

2. METHODS

2.1. Source of Data

The dataset for this project was obtained from a Kaggle repository titled *Dangerous Heartbeat Dataset (DHD)* [1], which in turn sources its data from the PASCAL Classifying Heart Sounds Challenge 2011 (CHSC2011) [3]. This dataset comprises audio recordings of heartbeats, categorized into different types of heart sounds. Specifically, the dataset consists of 5 types of recordings: Normal Heart Sounds, Murmur Sounds, Extra Heart Sounds, Extrasystole Sounds, and Artifacts. Data has been gathered from the general public via the iStethoscope Pro iPhone app and from a clinic trial in hospitals using the digital stethoscope DigiScope.

Type of Sources

The dataset comprises audio recordings collected from three distinct sources:

Type A: This subset includes recordings contributed by the general public through the iStethoscope Pro iPhone app. Users from diverse backgrounds and locations have submitted these recordings, providing a wide range of heart sounds in various conditions.

Type B: This subset consists of recordings obtained from clinical trials conducted in hospitals using the DigiScope digital stethoscope. These recordings are collected in controlled environments, contributing to a high-quality dataset for clinical applications.

Type C: This subset is a mixed collection that includes recordings from both the iStethoscope Pro app and the DigiScope digital stethoscope. Additionally, this subset incorporates heart sound recordings sourced from various publicly available datasets on the internet. This mixed dataset is valuable for its diversity and comprehensiveness, covering a broad spectrum of heart sound variations and abnormalities.

These diverse sources ensure a robust dataset that supports comprehensive analysis and improves the generalizability of the heartbeat audio classification model.

Classes

Heart sounds can be categorized into different classes based on their acoustic characteristics and clinical significance. Accurate classification of these sounds is essential for diagnosing and treating a variety of cardiac conditions. The primary categories include Normal heart sounds, Murmurs, Extra Heart Sounds, Artifacts, and Extra Systoles. Understanding the distinct features and clinical implications of each class is a crucial step before building a machine learning model to classify heartbeats. This phase is particularly important for the identification of patterns that are characteristic of specific classes, which in turn guides the selection of features to extract from the audio. This knowledge aids in identifying specific patterns and anomalies within the heart sounds, leading to more precise and reliable model predictions.

Normal The Normal category includes recordings of typical, healthy heart sounds. These sounds exhibit the characteristic “lub-dub, lub-dub” pattern, where “lub” (S1) represents the closing of the atrioventricular valves and “dub” (S2) signifies the closing of the semilunar valves. In a normal heart, the time interval between “lub” and “dub” is shorter than the interval from “dub” to the next “lub,” especially when the heart rate is below 140 beats per minute. Most normal heart rates at rest fall between 60 and 100 beats per minute, though rates can vary from 40 to 140 beats per minute based on factors such as age and activity level. Recordings may include background noises like traffic or radio sounds and may capture incidental noises such as breathing or microphone contact with clothing or skin. It contains both clean and noisy normal recordings, the latter featuring significant background noise or distortion, which simulates real-world conditions.

Figure 1 shows a sample of a normal heart beat audio. The characteristic “lub-dub, lub-dub” pattern can be observed, where the peaks represent the “lub” (S1) and “dub” (S2) sounds of a healthy heart.

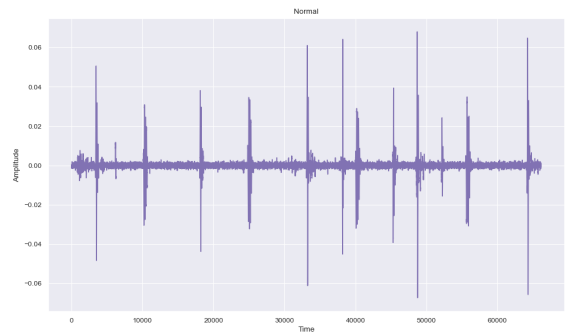


Fig. 1: Sample of normal heart beat audio.

Murmur Heart murmurs are abnormal sounds during the heartbeat cycle, such as a “whooshing, roaring, rumbling, or turbulent fluid” noise, heard between the “lub” and “dub” (systolic murmur) or between “dub” and “lub” (diastolic murmur). These murmurs are typically indicative of turbulent blood flow in the heart and can signal various heart conditions, some of which may be serious. It is

Authors	Models	Features	Results	Anno	Data
T. Alafif et al [2]	2D-CNN + transfer learning	MFCC	0.89 Accuracy	2020	N, A
Noman et al [9]	Ensemble CNN	1D time series + MFCC	0.89 Accuracy	2019	N, A
Rath et al [Rath_Mishra_Panda_Pal_2022]	Ensemble (RF + MFO + XGB + EL)	MFCC + DWT	0.87 Accuracy	2022	N, A
A. Raza et al [10]	LSTM	1D time series	0.80 Accuracy	2019	N, M
Chen et al [4]	2D CNN	WT + Hilbert-Huang	0.93 Accuracy	2018	N, M
W. Zhang et al [12]	SVM	Spectrogram	0.76 Precision	2017	N, M
SW. Deng et al [6]	SVM	DWT	0.76 Precision	2016	N, M
Our Model	Ensemble Model (MLPs + RF)	MFCC + Chroma + ZCR	0.88 Accuracy	2024	AR, ES

Table 1: Comparison of different models for classification. **Legend:** N: Normal, M: Murmur, EH: Extra Heartbeat, AR: Artifact, ES: Extra systoles, A: Abnormal

crucial to distinguish murmurs from the normal “lub-dub” sounds since they occur between the primary heart sounds and not concurrently with them. It also includes noisy murmur data, which mimics real-world recording scenarios by incorporating significant background noise and distortions. Figure 2 shows a sample of a murmur heart beat audio. The presence of additional sounds between the “lub” and “dub” peaks can be observed, indicating the characteristic “whooshing, roaring, rumbling, or turbulent fluid” noise typical of heart murmurs.

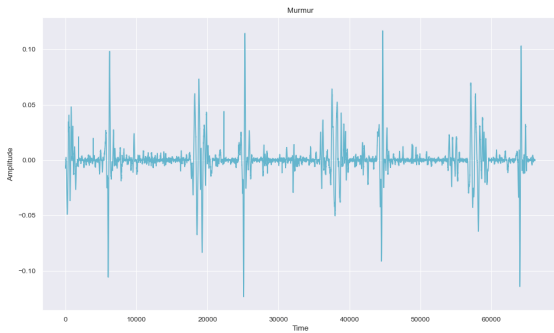


Fig. 2: Sample of murmur heart beat audio.

Extra Heart Sound Extra heart sounds are characterized by an additional sound in the cardiac cycle, producing patterns such as “lub-lub dub” or “lub dub-dub”. These sounds can arise from physiological or pathological conditions. For example, a third heart sound (S3) may indicate heart failure or volume overload, while a fourth heart sound (S4) can be associated with a stiff or hypertrophic ventricle. Detecting these extra sounds is important for identifying potential heart diseases early, allowing for timely intervention and management. Figure 3 shows a sample of an extra heart sound audio. The presence of additional peaks within the normal “lub-dub” pattern indicates extra heart sounds, which can be critical for diagnosing various heart conditions.

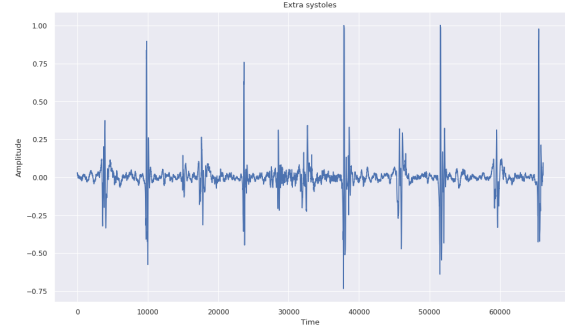


Fig. 3: Sample of extra heart sound audio.

Artifact The Artifact category consists of recordings with non-cardiac sounds, including feedback squeals, echoes, speech, music, and various types of noise. These recordings generally lack discernible heart sounds and do not exhibit the temporal periodicity typical of heartbeats at frequencies below 195 Hz. Accurately identifying artifacts is essential to avoid misinterpreting non-cardiac sounds as pathological heart sounds, ensuring that data collection efforts focus on genuine heart sounds. Figure 4 shows a sample of an artifact heart beat audio, there can be observed that there is not a clear pattern in the audio.

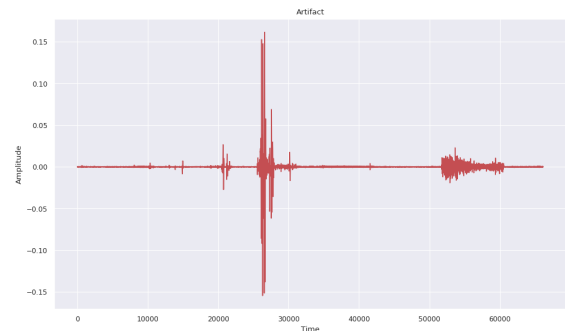


Fig. 4: Sample of artifact heart beat audio

Extra systoles Extra systoles refers to extra or skipped heartbeats, resulting in irregular patterns such as “lub-lub dub” or “lub dub-dub”. Unlike the regular extra heart sounds, extra systoles are sporadic and do not follow a consistent rhythm. These premature beats can occur in healthy individuals, particularly children, but they may also be associated with various heart diseases. Identifying extra systoles is crucial as they can be early indicators of cardiac conditions that might require medical attention if they occur frequently or in certain patterns.

In the audio signal depicted in Figure 5, irregularities

within the normal “lub-dub” pattern are evident. These irregularities manifest as additional peaks or skipped beats, indicating extra systoles.

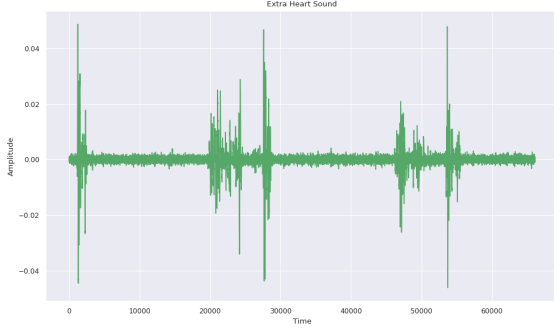


Fig. 5: Sample of extra systoles heart beat audio

Comparison of Heart Sounds In Figure 6, a comparison of the different classes of heart sounds can be observed.

As we can see, the “Artifact” signal appears erratic with no consistent pattern, likely representing noise or interference rather than true heart sounds.

The “Murmurs” signal shows irregular fluctuations in amplitude, which could indicate turbulent blood flow typically associated with murmurs.

The signal for “Extra Heart Beat Sound” has occasional spikes in amplitude that stand out from the baseline.

The “Normal” signal appears more uniform and regular compared to the others, reflecting the expected rhythm of a healthy heartbeat. Finally, the signal for “Extra Systoles” shows extra spikes at irregular intervals, indicating unexpected contractions of the heart muscle (systoles) occurring outside the normal rhythm.

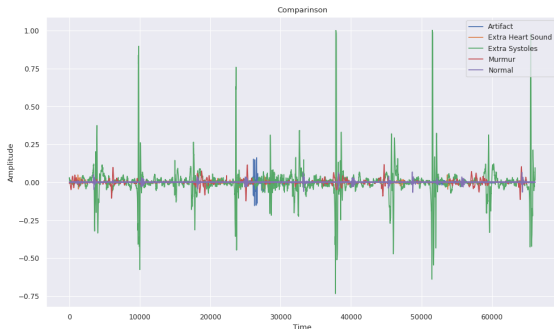


Fig. 6: Comparison of the different classes of heart sounds.

Data Distribution

Figure 7, illustrates the significant class imbalance present in the dataset, particularly for the ‘Extrastole’ and ‘Extrahls’ classes, which have far fewer samples compared to other classes. This imbalance poses a challenge for the classification task, as the model may struggle to learn and accurately predict the underrepresented classes due to the insufficient number of training examples. To mitigate this issue, several strategies are employed.

Data augmentation techniques are applied to artificially increase the size of the dataset by creating modified versions of the existing audio files through methods such as

pitch shifting, time stretching, and adding noise. Additionally, the original audio recordings are segmented into smaller clips, which not only increases the number of samples available for training but also provides the model with more varied examples of heart sounds, enhancing its ability to generalize across different heart sound variations.

Furthermore, the effectiveness of oversampling and undersampling techniques is tested. Oversampling involves duplicating samples from the minority classes to increase their representation in the training set, while undersampling involves reducing the number of samples from the majority classes to balance the dataset. The data is split into training and testing sets with an 80% - 20% ratio, respectively.

A validation set is omitted due to the low number of samples available, ensuring that the maximum amount of data is used for training and testing the model.

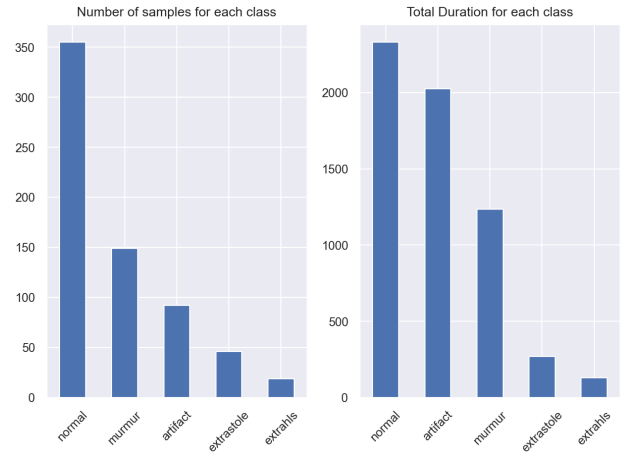


Fig. 7: Number of samples per duration.

2.2. Data Preprocessing

To prepare the data several preprocessing operations were performed:

Noise Reduction: the audio data was already provided in a clipped format to minimize noise and irrelevant information.

Normalization: the audio are loaded using the *torchaudio.load()* function, which normalized the audio signals in the range [-1, 1].

Removal of Corrupted Files: corrupted files were identified and removed from the dataset to ensure data quality.

Outlier Detection and Removal: we investigated the average duration of each class and found the ‘artifact’ class to have a significantly larger average duration. This was due to a few long lasting audio recordings (see Figure 8). A large number of samples from the same audio might not be as informative, thereby we used IQR to detect and remove outliers.

Resampling: we evaluated two sampling rates to determine the optimal rate for heartbeat sounds and all audio files were resampled to a common frequency of 4000 Hz (see Section 2.3).

Segmentation: the audio data was segmented into 1-second intervals, identified as the optimal extraction interval (see Section 2.3), as it offered both good performance and dataset size increasing.

Hop and Window Size: the hop size determines the number of samples between successive windows, while the window size determines the number of samples considered. Each feature was extracted using the same window length and hop length facilitating a fair assessment of each feature's contribution to the classification task.

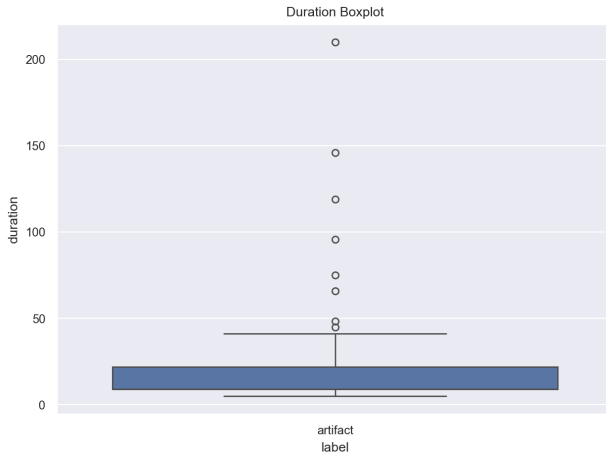


Fig. 8: Outliers in the Artifacts class.

2.3. Feature Extraction

As demonstrated by [10] and [5], MFCCs are highly effective features for heartbeat classification. In addition to MFCCs, we incorporated other features to capture various characteristics of heart sounds, enhancing the classification accuracy. The features used are explained in the following section.

Features Type

MFCC

Mel-Frequency Cepstral Coefficients (MFCCs) are representations of the short-term power spectrum of sound. They are derived by taking the Fourier transform of a signal, mapping the powers of the spectrum onto the mel scale, taking the logarithm, and then performing a discrete cosine transform. MFCCs are effective in capturing the timbral texture of audio and are widely used in speech and audio processing due to their ability to represent the envelope of the time power spectrum. In heartbeat classification, MFCCs can reflect the different perceived quality of heart sounds, such as the presence of murmurs or other anomalies.

Chroma STFT

Chroma features represent the 12 different pitch classes of music (e.g., C, C#, D, etc.). They are particularly useful for capturing harmonic and melodic characteristics in music. By mapping audio signals onto the chroma scale, these features can identify pitches regardless of the octave, making them useful for analyzing harmonic content in heart

sounds.

RMS

Root Mean Square (RMS) measures the magnitude of varying quantities, in this case, the amplitude of an audio signal. It is a straightforward way to compute the energy of the signal over a given time frame. RMS is useful in audio analysis for detecting volume changes and can help identify different types of heartbeats based on their energy levels. For example, in a given timeframe the RMS may be altered by the presence of a murmur with respect to a normal heart sound.

ZCR

Zero-Crossing Rate (ZCR) is the rate at which a signal changes sign, indicating how often the signal crosses the zero amplitude line. It is particularly useful for detecting the noisiness and the temporal structure of the signal. In heartbeat classification, ZCR can help differentiate between normal and abnormal sounds by highlighting changes in signal periodicity.

CQT

Constant-Q Transform (CQT) is a time-frequency representation with a logarithmic frequency scale, making it suitable for musical applications. Since it captures more detail at lower frequencies, it may be useful for analyzing the low-frequency components of heart sounds.

Spectral Centroid

The spectral centroid indicates the center of mass of the spectrum and is often perceived as the brightness of a sound. It is calculated as the weighted mean of the frequencies present in the signal, with their magnitudes as weights. In heart sound analysis, a higher spectral centroid can indicate sharper, more pronounced sounds, while a lower centroid suggests smoother sounds.

Spectral Bandwidth

Spectral bandwidth measures the width of the spectrum around the centroid, providing an indication of the range of frequencies present. It is calculated as the square root of the variance of the spectrum. This feature helps in understanding the spread of the frequency components in the heart sounds, which can be indicative of different heart conditions.

Spectral Roll-off Spectral roll-off is the frequency below which a certain percentage of the total spectral energy lies. It is typically set at 85% and helps distinguish between harmonic and non-harmonic content. In heartbeat classification, spectral roll-off can be used to differentiate between sounds with a concentrated energy distribution and those with more dispersed energy.

Sampling Rate Selection

The sampling rate of the data were heterogeneous, ranging from 4000 Hz to 44100 Hz, with a majority of the data being sampled at 4000 Hz. To assess the impact of the sampling rate on the classification performance, we trained

different models on different features, extracted at different sampling rates and from various intervals. Each model is then evaluated using different metrics, taking into account the class imbalance issue. We also considered a possible dependency between the sampling rate and the extraction interval, as shown in Algorithm 1.

Algorithm 1 Sampling rate and Interval choice

```

1: Input:
2: features = [mfcc30 & 120, cqt30 & 70, chroma12]
3: sampling_rates = [mix, 4000]
4: extraction_intervals = [0.5, 1, 2, 3]
5: models = [rf, svm-rbf, lr]
6: metrics = [macrof1, mcc]

7: for sr in sampling_rates do
8:   for interval in extraction_intervals do
9:     for feature in features do
10:      extract feature with interval at sr
11:      for model in models do
12:        train model with extracted feature
13:        for metric in metrics do
14:          evaluate model with metric
15: Output:
16: Given all the results, group by model and average the values
    of a specific metric across features
  
```

The results, reported in Figure 9 showed no evident advantage to using a mix of sampling frequencies over a fixed resampled sample rate. Moreover, employing a fixed sample rate of 4000 Hz reduces the risk of introducing bias, enhances efficiency, and permits the use of a broader range of features and models.

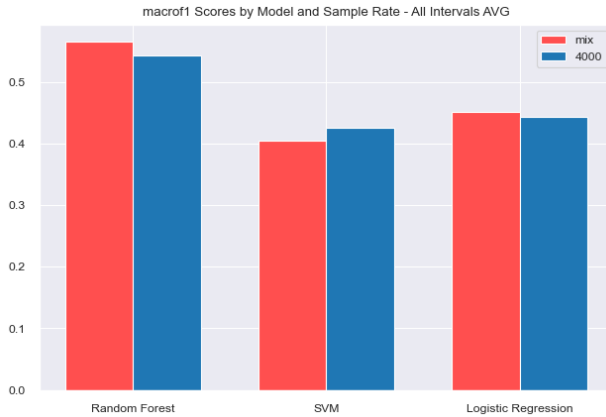


Fig. 9: Comparison of the macro F1 score for different sampling rates.

Extraction Interval Selection

The extraction interval refers to the duration of the audio segment from which the features are extracted. Using algorithm 1, we evaluated the performance of 0.5, 1, 2, and 3-second intervals on the classification task. It is important to note that the interval choice affects the number of samples available for training and evaluation, so in case of a limited number of samples, this choice should not be based solely on the performance of the model. The results, showed that a 2-second interval yielded the best performance, however it also reduced the number of samples, impeding a correct

training and evaluation of the models. As a consequence, we picked a 1-second interval as a compromise.

Number of Features per Type

Now the focus, the focus is on identifying the optimal number of features for different types of audio features (MFCC, Chroma, CQT, etc.). Each type of feature can consist of a varying number of individual features, and it is crucial to determine the optimal number to maximize the model's performance. Proper feature selection is vital because it directly impacts the efficiency, accuracy, and generalizability of the machine learning model. Including too many features can lead to overfitting, increased computational costs, and degraded performance due to the curse of dimensionality. On the other hand, using too few features can result in underfitting, where the model fails to capture the necessary patterns in the data. Therefore, the goal of this study is to identify the optimal number of features for each type to ensure the model is both robust and efficient.

Determining the Optimal Number of Features To maximize the model's performance, it is crucial to determine the optimal number of features for each type. This was achieved using a 'One Model per Feature' approach, which involved the following steps:

Algorithm 2 Feature Optimization Process

- 1: **Step 1:** Extract feature sets with varying sizes: 12, 20, 30, 40, 60, 70, 90, and 120 features.
 - 2: **Step 2:** Train a separate model for each feature type and feature set size.
 - 3: **Step 3:** For each feature set, train three different models using three classifiers: SVM, Random Forest, and Logistic Regression.
 - 4: **Step 4:** Evaluate the performance of each model.
-

Figure 10 shows the results obtained for each type of feature with the Random Forest model, which significantly outperformed the other classifiers. From the figure, we can observe the following trends for each feature type:

- **MFCC:** The MFCC features consistently achieved the highest F1 scores, peaking around 0.7. This indicates their effectiveness for the classification task. Interestingly, the number of MFCC features (ranging from 30 to 120) did not drastically affect performance, suggesting that even a smaller set of MFCC features can be highly informative.
- **CQT:** The CQT features showed moderate performance, with F1 scores around 0.4 to 0.5. The optimal number of features was around 70, beyond which there was no significant improvement.
- **RMS:** RMS features exhibited F1 scores ranging from 0.4 to 0.5, with optimal performance achieved with around 70 features.
- **ZCR, Spectral Centroid (SC), Spectral Bandwidth (SB), and Spectral Roll-off (SR):** The F1 scores for

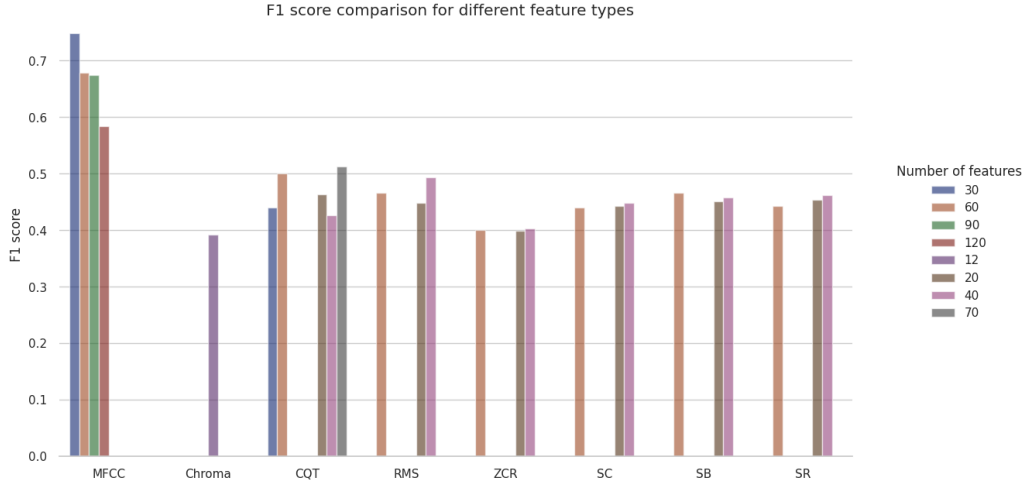


Fig. 10: F1 score per number of features

these features generally stabilized around 0.4 to 0.5. Increasing the number of features beyond 40 did not result in significant performance gains and could even degrade the model's performance. This suggests that adding too many features, especially those without strong predictive power, can confuse the model and degrade its performance.

Optimal Number of Features Based on the results, the optimal number of features for each type is shown in Table 2.

Feature Type	Optimal Number of Features
MFCC	30
Chroma	12
CQT	70
RMS	40
ZCR	40
Spectral Centroid	40
Spectral Bandwidth	60
Spectral Roll-off	40

Table 2: Optimal number of features for each type

2.4. Feature Selection

Given the large number of features (338 in total), it was necessary to identify and remove features that are poorly correlated with the target variable as well as those that are highly correlated with each other. Due to the high number of features, a visual approach, such as a correlation matrix, was not feasible. Instead, two filters were applied to select the most relevant features using the Spearman correlation coefficient, as the normality test failed.

The first filter is based on the correlation between the features and the target variable. Features with a correlation below a certain threshold with the target variable are removed.

The second filter focuses on the correlation among the features themselves. It counts, for each feature, the number of other features with which it has a correlation above a certain threshold. Features with a number of correlations

above a specified threshold are then removed.

Algorithm 3 Feature Selection Process

- Step 1:** Compute the normal test (D'Agostino Pearson).
- Step 2:** Compute the Spearman correlation coefficient for each feature with the target variable.
- Step 3:** Apply the first filter to remove features with a correlation below a certain threshold with the target variable.
- Step 4:** Compute the correlation matrix among all features.
- Step 5:** Apply the second filter to remove features that have a high number of correlations (above a certain threshold) with other features.
- Step 6:** Choose threshold values empirically and apply the filters using various combinations of these thresholds.
- Step 7:** Train Random Forest models on the filtered data to evaluate performance and select the best combination of thresholds.

Threshold Selection and Model Evaluation

Threshold values were chosen empirically and the filters were applied using the combinations shown in Table 3. Using the filtered data, Random Forest models were trained and evaluated, as Random Forest was found to be the best performing model. The optimal combination of thresholds was found to be: threshold 1 = 0, threshold 2 = 0.6 and number of features = 30, resulting in 30 features.

Threshold	Values
THRESHOLD 1	0 - 0.1 - 0.2 - 0.3 - 0.4 - 0.5
THRESHOLD 2	0.6 - 0.7 - 0.8 - 0.9 - 1
N° FEATURES	5 - 10 - 15 - 20 - 25 - 30 - 40

Table 3: threshold values

With threshold 1 = 0, the filter on the correlation between the features and the target variable was effectively by-

passed. However, with threshold 2 = 0.6, a stringent filter was applied on the correlation among the features themselves, removing features that had a correlation above 0.6 with at least 30 other features. This indicates that having features highly correlated with each other is more detrimental to the model than having features poorly correlated with the target variable.

Figure 11 shows the results obtained with the model trained on filtered features compared to the model trained on all features. As demonstrated, the model trained on filtered features performs significantly better.

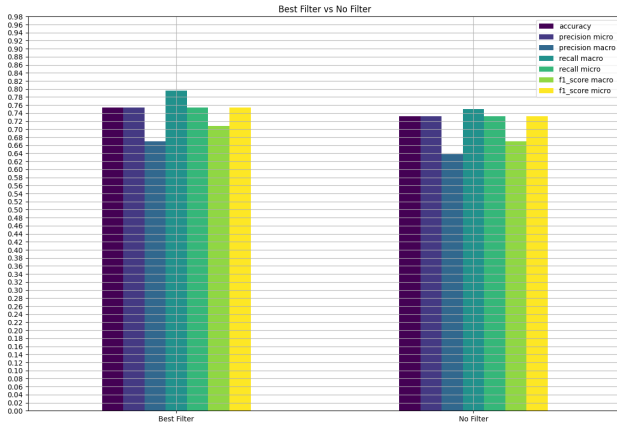


Fig. 11: Comparison of different metrics between the model on all features and the model on the filtered ones

Selected Features and Correlation Matrix

From this analysis, 41 features remained: 28 MFCC, 12 Chroma, and 1 ZCR. The correlation matrix of the filtered features is shown in Figure 12. This matrix illustrates the pairwise correlation between the selected features, with the color intensity indicating the strength and direction of the correlation. Dark red cells represent high positive correlations, while dark blue cells indicate high negative correlations.

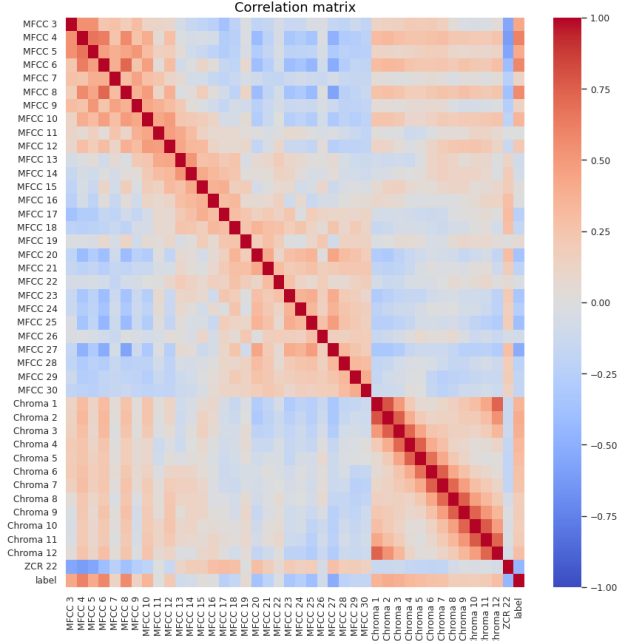


Fig. 12: Correlation matrix of the filtered features

The matrix demonstrates that the remaining features have low correlations with each other, as evidenced by the predominantly light colors away from the diagonal. This implies that the features are relatively uncorrelated, preventing multicollinearity issues and enhancing the robustness of the model. The high diagonal values indicate that each feature is perfectly correlated with itself, which is expected. However, the off-diagonal values being close to zero for most feature pairs confirm that the filtering process was effective in selecting features that do not exhibit high inter-correlations.

2.5. Models

Metrics

In this project, various metrics evaluate the heartbeat audio classification model, focusing on multiclass classification with imbalanced classes.

Accuracy Accuracy measures the ratio of correct predictions to the total number of predictions:

$$\text{Accuracy} = \frac{\text{Correct Predictions}}{\text{Total Predictions}}$$

It is straightforward but can be misleading with imbalanced classes.

Balanced Accuracy Balanced accuracy addresses class imbalance by averaging recall across classes:

$$\text{Balanced Accuracy} = \frac{1}{N} \sum_{i=1}^N \frac{TP_i}{TP_i + FN_i}$$

where N is the number of classes, TP_i is true positives, and FN_i is false negatives for class i .

Matthews Correlation Coefficient (MCC) MCC evaluates performance by considering all classes:

$$MCC = \frac{\sum_k \sum_l \sum_m C_{kk} C_{lm} - C_{kl} C_{mk}}{\sqrt{\sum_k (\sum_l C_{kl}) (\sum_{l' \neq k} \sum_{l''} C_{k'l''})} \sqrt{\sum_k (\sum_l C_{lk}) (\sum_{l' \neq k} \sum_{l''} C_{l'k})}}$$

This comprehensive metric accounts for true and false predictions, making it robust for imbalanced datasets.

Precision and Recall Precision measures the accuracy of positive predictions:

$$\text{Precision} = \frac{TP}{TP + FP}$$

Recall measures the proportion of actual positives correctly identified:

$$\text{Recall} = \frac{TP}{TP + FN}$$

Micro variants aggregate these metrics across all classes, while macro variants average them per class, offering insights into individual class performance.

F1 Score The F1 score balances precision and recall:

$$\text{F1 Score} = 2 \times \frac{\text{Precision} \times \text{Recall}}{\text{Precision} + \text{Recall}}$$

Micro and macro variants provide overall and class-specific performance evaluations, respectively.

ROC Curve and AUC For binary classification, the ROC curve plots true positive rate against false positive rate, and AUC summarizes the model's discriminatory ability, with higher AUC indicating better performance.

Risk Score The risk score evaluates the model's ability to avoid misclassifying heart disease as normal:

$$\text{Risk score} = \frac{FP}{FP + TP}$$

A lower risk score indicates better performance. Disease-specific risk scores can provide detailed insights into different heart conditions.

Prevention Model

The goal of the prevention model is to provide an accessible tool for the early diagnosis of heart diseases, potentially usable by non-experts. Therefore, it is crucial to develop a model that minimizes the number of false normal predictions to accurately indicate the presence or not of disease or identify artifacts in the provided data.

To achieve this, different heart diseases were grouped together, transforming the problem into a 3-class classification task: normal, disease, and artifact. Grouping the diseases not only simplified the classification but also balanced the class distribution. The data was divided into training and testing sets in an 80-20 ratio, and various models were evaluated, as shown in Table 4.

The primary metrics for evaluating the models were the ROC-AUC score, false positive rate (FPR), and true positive rate (TPR), with F1-score and accuracy as secondary metrics. To adapt binary metrics for multi-class classification, the one-vs-rest strategy was employed. Specifically, we focused on the normal-vs-rest case to minimize false normal predictions.

In summary, each model was trained on the 3-class classification problem but was evaluated based on its binary classification performance (normal-vs-rest). The best model was selected based on its ROC-AUC score and performance at specific FPR levels (1%, 5%, 10%, and 20%). The objective was to minimize false normal predictions while maximizing true normals. A model predicting no cases as normal to achieve a 0% FPR would be ineffective.

Support Model

In addition to the Prevention model, we developed a complementary model designed to assist clinicians in diagnosing heart diseases. This model aims to accurately classify all classes present in the dataset, avoiding any simplifications, to ensure comprehensive diagnostic support.

Given the highly imbalanced nature of the dataset, where certain classes contain significantly fewer samples, traditional accuracy metrics can be misleading. To address this, we explored various balancing techniques, but they did not yield satisfactory results. Consequently, we prioritized metrics that provide equal importance to all classes, including the macro F1-score, balanced accuracy, and Matthews Correlation Coefficient (MCC). These metrics collectively offer a robust evaluation by accounting for class imbalance, ensuring that minority classes receive adequate consideration alongside majority classes.

A particular emphasis was placed on the 'Normal' class, focusing on minimizing false positives. This is crucial for patient safety, as misclassifying abnormal heart sounds as normal could lead to missed diagnoses and delayed treatment. To address this concern, we introduced a 'Risk score' that quantifies the impact of normal false positives, allowing the model to be more sensitive to this critical aspect. This score was further adapted to evaluate individual diseases, enhancing our ability to assess the model's risk for each specific condition.

The selection of the best model was guided by the macro F1-score and balanced accuracy. These metrics comprehensively reflect performance across all classes, ensuring that no disease category is overlooked. After identifying the optimal model, we employed explainability techniques to elucidate the model's decision-making process. This step is crucial because the model's outputs directly impact patient care; therefore, transparency and interpretability are essential. By providing clinicians with insights into how the model arrives at its conclusions, we enhance trust and facilitate informed clinical decisions.

To achieve this, we computed feature importance using Permutation Feature Importance, which, according to A. Fisher et al.[7], highlights the most influential factors driving the model's predictions.

Additionally, we applied SHAP (SHapley Additive exPlanations) values, introduced by Scott M. Lundberg and Su-In Lee [8], to interpret the model’s output at the individual prediction level. SHAP values provide a detailed breakdown of each prediction, illustrating the impact of specific features on the model’s decision. Based on the SHAP values, we identified the areas in the audio signal that significantly influenced the model’s classification.

By integrating these explainability techniques, we ensure that the model’s decision-making process is transparent and comprehensible. This not only builds confidence among clinicians but also ensures that the model’s outputs are actionable and reliable in a clinical setting.

2.5.1. Experimented Architectures

Name	Architecture (hidden layers)
Random Forest	-
XGBoost	-
CatBoost	-
LightGBM	-
MLP_Basic	(128, 64, 32)
MLP_Ultra	(512, 256, 128, 64, 32)
MLP_Large	(256, 128, 64, 32)
MLP_Small	(64, 32)
MLP_Tiny	(32, 16)
MLP_Reverse	(32, 64, 128, 256, 512, 256, 128, 64, 32)
MLP_Bottleneck	(512, 64, 32)
MLP_Rollercoaster	(512, 128, 256, 128, 256, 64, 32)
MLP_Hourglass	(512, 256, 128, 64, 32, 64, 128, 256, 512)
MLP_Pyramid	(1024, 512, 256, 128, 128, 128, 64, 32)
MLP_Wide	(1024, 1024)
MLP_WideUltra	(1024, 1024, 128, 32)
MLP_Sparse	(32, 16, 8)
MLP_Dropout	(128, 64, 32)
MLP_Ensemble1	MLP_Basic, Large, Ultra
MLP_Ensemble2	RandomForest, MLP_Ultra
MLP_Ensemble3	MLP_Rollercoaster, Large
MLP_Ensemble4	MLP_Rollercoaster, Large, Ultra
MLP_Ensemble5	RandomForest, MLP_Ultra, Rollercoaster
MLP_Ensemble6	MLP_Rollercoaster, Large, Ultra, Wide
ALL_Ensemble	All models majority vote
CB_ALL_Ensemble	All models CatBoost

Table 4: Models names and architectures.

The architectures of the models used in the experiments are detailed in Table 4. Special attention is given to the ensemble models, which combine predictions from multiple models to enhance overall performance.

All MLP_Ensemble models consist of the individual models listed in their architecture name. These models’ predictions are combined using a soft voting strategy, where the final prediction is determined by the argmax of the sum of the predicted probabilities from each model. This approach is effective when the models are well-calibrated and exhibit complementary strengths and weaknesses.

The ALL_Ensemble model aggregates the predictions of all individual models using a majority vote strategy. In contrast, the CB_ALL_Ensemble model also considers all individual models but uses a CatBoost model to aggregate the predictions. This allows for a more flexible voting strategy, potentially leading to improved performance.

2.6. Tools and Software

This study utilized several powerful libraries and tools for data processing, model training, and evaluation:

- **Scikit-learn:** Used for MLP, RF, and metrics such as F1, Balanced Accuracy, Accuracy, MCC, ROC, AUC, permutation importance, train-test split, confusion matrix and voting classifiers.
- **Torchaudio:** Used to load the audio, for MFCC extraction and audio resampling.
- **Librosa:** Used for other features extraction and audio processing and augmentation.
- **Imblearn:** Applied for handling imbalanced datasets with techniques such as undersampling, oversampling, and SMOTEN.
- **Numpy:** Essential for numerical computations and array manipulations.
- **Pandas:** Crucial for data manipulation and analysis.
- **Matplotlib:** Employed for creating visualizations.
- **Seaborn:** Used for statistical data visualization.
- **Scipy:** Utilized for scientific and technical computing.
- **XGBoost:** Implemented for gradient boosting models.
- **CatBoost:** Applied for gradient boosting on decision trees.
- **PyTorch:** Used for developing and training CNN models, specifically VGG16_bn.
- **TensorFlow:** Used for building and training deep learning models, including CNNs.
- **Keras:** High-level API for building and training neural networks on TensorFlow.
- **Shap:** Utilized for model interpretability.
- **Other Utility Libraries:** Includes `joblib` for model serialization, and `os`, `sys` for system operations and file handling.

3. RESULTS

3.1. Prevention Model

The initial evaluation is presented using the ROC curves of the normal class versus the others for selected models. According to Figure 13, the MLP models outperformed the other models, as indicated by the higher AUC values. Specifically, *MLP_Ensemble5* achieved the highest AUC value of 0.96, followed by *MLP_Ultra*, *MLP_Rollercoaster*, *MLP_Ensemble2*, and *MLP_Ensemble4*, all with an AUC of 0.95.

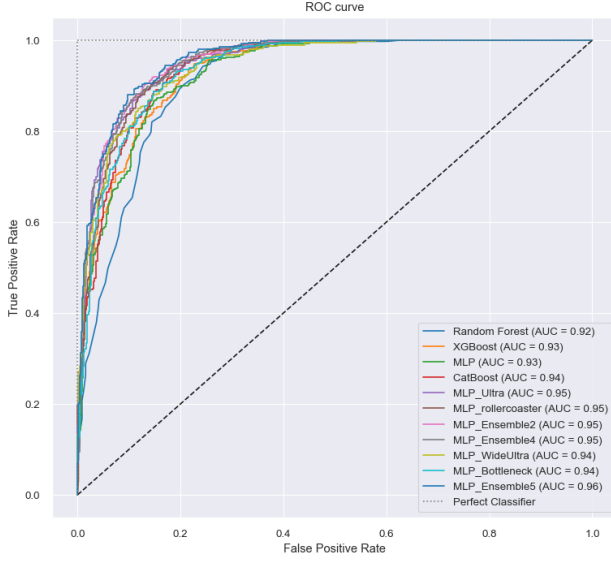


Fig. 13: ROC curves for the normal class against the rest of the classes across all models.

To further analyze model performance, we selected four significant FPR levels (1%, 5%, 10%, 20%) and calculated the corresponding TPR. The consolidated results are shown in Figure 14.

At each FPR level, *MLP_Ensemble5* outperformed the other models, achieving TPRs of 43.4%, 74.3%, 86.6%, and 95.8% at the 1%, 5%, 10%, and 20% FPR levels, respectively. Excluding *MLP_Ensemble5*, the best-performing model varied by FPR level: *MLP_WideUltra* at 1%, *MLP_Ultra* at 5%, *MLP_Ensemble2* at 10%, and *MLP_Ensemble4* at 20%.

These outcomes highlight the task’s challenges in creating a model that performs well across all FPR levels and demonstrate the efficacy of a well-built ensemble model, which leverages the strengths of different models to achieve optimal performance.

Best Model Analysis

To understand the performance of the ensemble model (detailed architecture depicted in Figure 25), we compared its confusion matrix against the confusion matrices of the individual models that compose it (Figure 15).

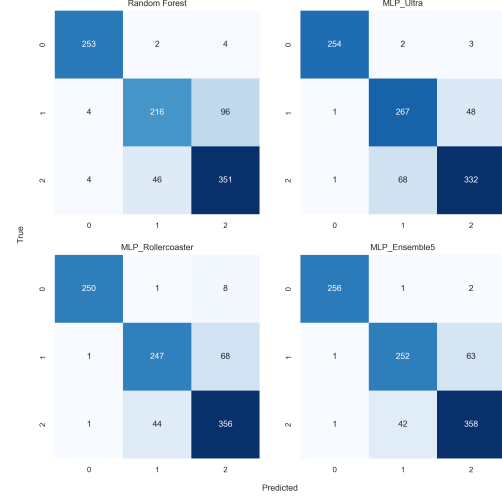


Fig. 15: Confusion matrices of the individual models and the ensemble model.

In the confusion matrix, class 2 represents normal heartbeats, class 1 represents abnormal heartbeats, and class 0 represents artifacts. The Random Forest and MLP_Ultra models exhibit complementary strengths: the Random Forest works better in recognizing normal samples, while the MLP_Ultra model performs better in identifying abnormal samples. The ensemble model effectively combines these strengths.

The contribution of the MLP_Rollercoaster model to the ensemble’s performance is less apparent but has been experimentally demonstrated. This may be due to its ability to correctly classify some samples that are misclassified by the other models.

Notably, the MLP_Ultra model classifies fewer abnormal heartbeats as normal compared to the MLP_Ensemble5 model. However, this is because the MLP_Ultra model simply classifies fewer samples as normal. Minimizing the false positive rate (FPR) for the normal class by classifying all samples as abnormal would result in a very low true positive rate (TPR) for the normal class. This highlights the importance of analyzing FPR and TPR together.

In conclusion, the ensemble model is the most effective for classifying normal heartbeats, abnormal heartbeats, and artifacts, achieving an optimal trade-off between FPR and TPR.

3.2. Support Model

The support models are evaluated using several metrics, including macro F1 score, accuracy, balanced accuracy, and MCC. The results are depicted in Figure 16.

From the figure, it is evident that accuracy tends to be higher than other metrics for all models, indicating a potential bias as it overestimates model performance.

Among the models, the MLP ensembles generally show superior performance compared to individual models. Notably, the MLP_Ensemble2 model exhibits the highest performance, with a macro F1 score of 81.58 and an MCC of 81.53. This suggests that ensemble models effectively leverage the strengths of individual models to achieve optimal performance.

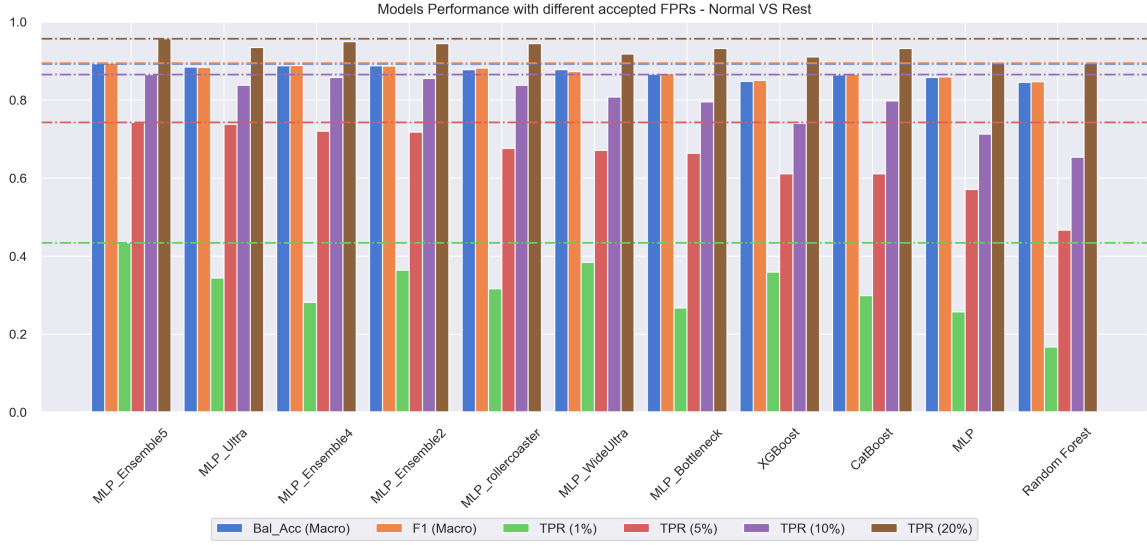


Fig. 14: TPR at different FPR levels for all models.

Model	Test Acc	Macro F1	Balanced Accuracy	MDC
XGBoost	83.71	71.16	62.17	76.70
CatBoost	85.14	74.29	72.85	78.79
LightGBM	84.12	72.58	69.74	77.30
MLP_Basic	82.99	77.83	77.44	75.39
MLP_Ultra	80.68	81.39	80.02	80.76
MLP_Large	84.82	76.41	76.02	77.34
MLP_Small	81.66	72.15	70.77	73.41
MLP_Tiny	79.71	68.25	67.11	70.60
MLP_Reverse	81.97	73.20	74.26	73.93
MLP_Bottleneck	85.86	76.36	75.27	79.51
MLP_Rollercoaster	84.52	76.71	77.30	77.40
MLP_Hourglass	84.84	72.56	72.17	78.08
MLP_Pyramid	85.45	76.06	75.57	78.97
MLP_Wide	84.53	75.97	75.70	77.54
MLP_WideUltra	83.81	73.53	71.19	76.61
MLP_Sparse	81.76	63.96	63.57	73.44
MLP_Dropout	81.86	70.30	69.57	73.65
MLP_Ensemble1	85.86	79.71	79.14	79.67
MLP_Ensemble2	87.19	81.58	79.23	81.53
MLP_Ensemble3	85.04	77.78	76.96	78.34
MLP_Ensemble4	89.27	78.25	77.43	80.12
MLP_Ensemble5	87.81	80.61	78.63	81.22
MLP_Ensemble6	86.89	79.65	77.72	80.98
ALL_Ensemble	87.50	80.88	78.63	81.90
CatBoost_ALL_Ensemble	87.91	79.62	78.52	82.48

Fig. 16: Metrics of the Support Models, computed on the test set

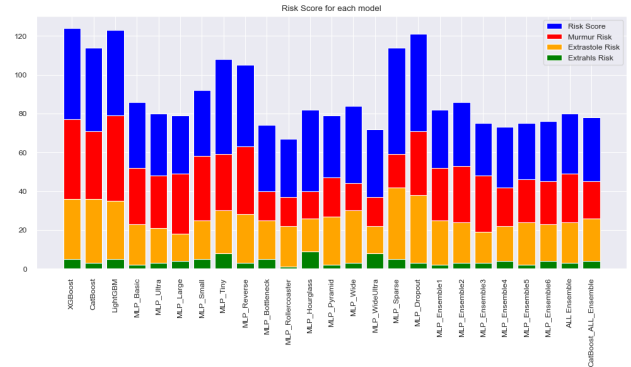


Fig. 17: Risk Scores of the Support Models

Best Model

The MLP_Ensemble2 model stands out as the best-performing model among the support models. To thoroughly understand its performance, we computed the confusion matrix on the test set, which is depicted in Figure 18. The confusion matrix reveals that the model excels in recognizing artifacts (class 0) and extra systoles (class 1). However, it tends to confuse murmurs (class 2) and extra systoles (class 4) with normal heartbeats (class 3).

The risk of misclassifying an abnormal sample as normal is depicted in Figure 17, which shows the overall risk scores (in blue) for each model. The graph also displays specific risk scores associated with each class, representing the probability of predicting a sample of that class as normal. This stacked bar chart helps compare the height of the different colors rather than their areas. From the figure, it's clear that no single model consistently outperforms others across all scores, but the performance varies across the scores. For instance, MLP_Rollercoaster has the best overall risk score (blue) and excels in murmurs risk score (red), while MLP_Ensemble3 performs best for extra systoles risk (orange).

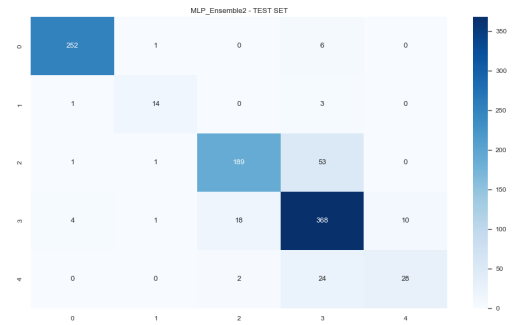


Fig. 18: Confusion Matrix of the MLP_Ensemble2 model. Columns represent the true classes, while rows represent the predicted classes. Class 0: Artifacts, Class 1: Extra heartbeats, Class 2: Murmurs, Class 3: Normal, Class 4: Extra systoles.

To further investigate this anomaly, we analyzed the mean values of the features within each class, as shown in Figure

19. The mean values represent the centroids of the classes in the feature space, providing insights into the distribution of the classes.

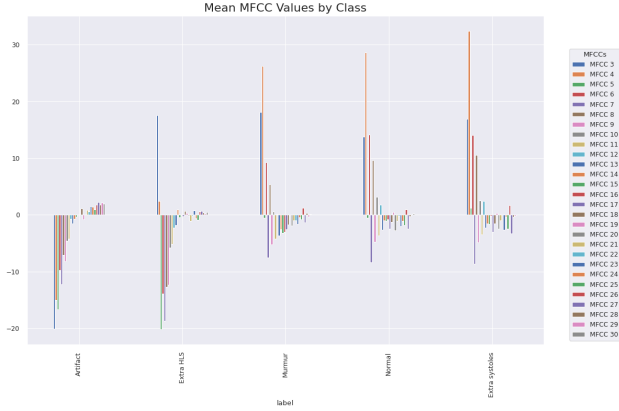


Fig. 19: Mean values for each feature within each class

The analysis indicates that artifacts and extra heartbeats have distinctly different mean values compared to other classes, while murmurs, extra systoles, and normal heartbeats exhibit similar mean values. To visualize this better, we employed T-SNE to map the features into a 2D space, as shown in Figure 20.

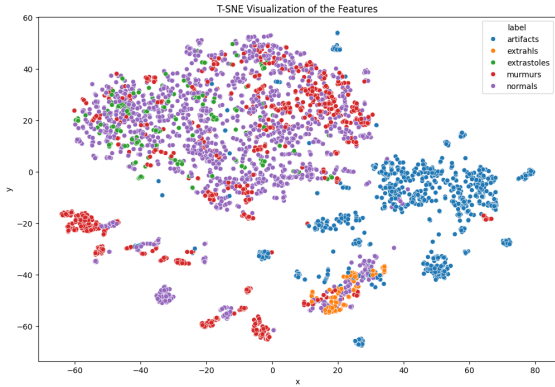


Fig. 20: T-SNE visualization of the features

The T-SNE visualization confirms the clear separation between artifacts and extra heartbeats from the other classes, while murmurs, extra systoles, and normal heartbeats are overlapped. This suggests that the features employed are not sufficiently distinct to differentiate normal heartbeats from murmurs and extra systoles, explaining the model's tendency to confuse these classes.

Explainability

To gain insights into the model's decision-making process, we computed the feature importance using permutation importance, as shown in Figure 21. The figure reveals that the most important features are the MFCCs, particularly MFCC 3, 4, 8, and 6. The fact that the lower MFCCs are most important, suggest that the to distinguish between classes the model doesn't require fine details of the audio signal. Surprisingly, the zero crossing rate and chroma features are less important, indicating that the model relies heavily on the MFCCs to make predictions.

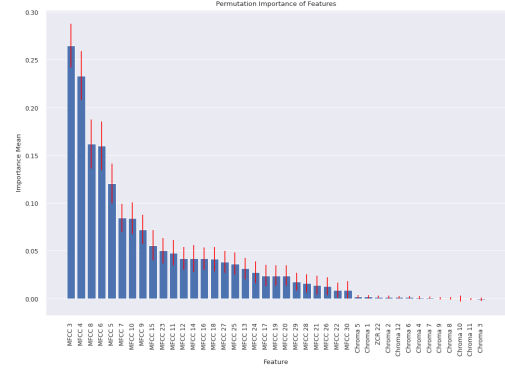


Fig. 21: Feature Importance computed with Permutation Importance

To provide a more intuitive understanding of the model's decision-making process, especially for clinicians who may need an explanation of the model's decisions, we identified the areas of the waveform most important for the model's prediction. This was done by first identifying the most important features for the classification of a single sample.

Once the most important MFCCs were identified, we plotted the waveform of the sample along with these MFCCs. By observing the values of the MFCCs, we can pinpoint the areas of the waveform that are critical for the model's decision. Figures 22 and 23 illustrate this process for a single extra heartbeat sample.

For this sample, the most important features are MFCC 8, 6, and 3. The bar plot shows that MFCC 8 and 6 have negative values, while MFCC 3 has a positive value, indicating that the significant areas of the waveform are where MFCC 3 is high and the others are low.

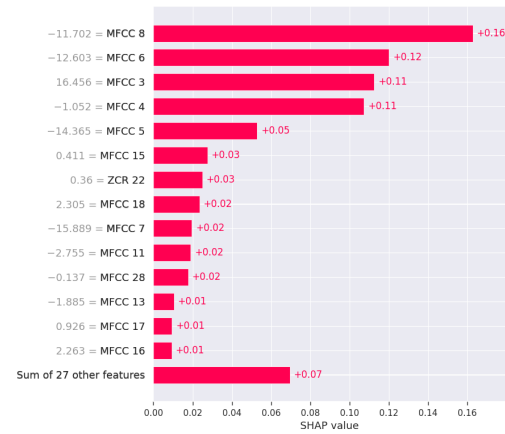


Fig. 22: Feature importance for a single extra heart beat sample

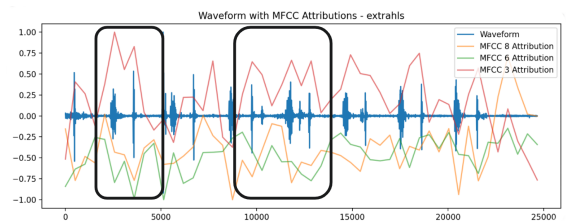


Fig. 23: Waveform of an extra heart beat sample, with most important MFCCs

3.3. Other Experiments

To further explore the classification problem, we conducted additional experiments involving CNN-based feature extraction, data augmentation, and a novel approach using a tiered ensemble model.

CNN-Based Experiments

We conducted a series of experiments using Convolutional Neural Networks (CNNs) to explore their effectiveness as feature extractors for the 5-class classification problem. The CNN was used with ImageNet weights and was not fine-tuned.

- **VGG16 with Spectral Features:** VGG16 CNN was employed as a feature extractor with spectral features (MFCC, CQT, Chroma STFT, among others) used as input images. This approach yielded a Macro F1 score of approximately 65%, which is lower than the performance achieved in the primary work.
- **VGG16 with Raw Waveform Images:** VGG16 was also used to extract features from raw waveform images. Features were taken from the 5th, 4th, and 3rd convolutional layers after pooling, and various classifiers (RF, SVM, MLP) were tested on these features. This method resulted in a performance of around 67%.

Data Augmentation

We explored data augmentation techniques to address the limited and imbalanced dataset and improve the model's generalization capabilities.

- **Noise Addition and Speed/Pitch Alteration:** We augmented the data by adding random noise (factor 0.05) and altering speed and pitch. However, the improvement in performance was not significant. This may be due to the limited size and inherent imbalance of the dataset, as data augmentation did not alter the class distribution.
- **Synthetic Data Generation with SMOTEN:** Synthetic data generation was applied to the less represented classes using SMOTEN. Although there was an initial spike in performance metrics, this was identified as bias. The model could easily distinguish the synthetically generated data from the original data. The underlying issue was the limited size of the original dataset, which did not provide sufficient variability for the synthetic generation algorithm to produce realistic and diverse samples.

Tiered Ensemble Model

We attempted to decompose the classification problem into two sub-problems, according to Figure 24.

- **Sub-problem 1: Artifact, Normal, and Abnormal Classification:** Various models were tested for distinguishing between artifact, normal, and abnormal audio. The best model (MLP_Ensemble5) achieved a balanced accuracy of approximately 89.2%.

- **Sub-problem 2: Disease Classification:** Different models were also applied to distinguish between different diseases, achieving a balanced accuracy of more than 90.3% with MLP_Ensemble2.
- **Final Ensemble Model:** A third model (CatBoost) was used to integrate the predictions from the above sub-problems and make the final classification among the five classes. This ensemble approach resulted in a balanced accuracy of 80.5%.

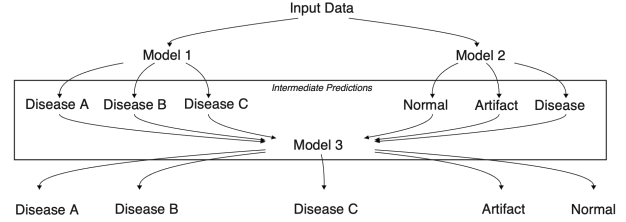


Fig. 24: Tiered Ensemble Model

Despite the promising results, the tiered ensemble model did not outperform the primary models.

4. DISCUSSION

In our research, we developed two ensemble models, MLP_Ensemble5 and MLP_Ensemble2, to address the dual purpose of enhancing prevention and diagnosis (support model) of heart disease. For MLP_Ensemble5, our focus was on minimizing false normals, ensuring that potential heart diseases are not overlooked. On the other hand, MLP_Ensemble2 aimed to maximize overall predictive performance while incorporating explainability to provide valuable insights to medical professionals.

Our experimentation involved various models and features, with careful consideration of correlation aspects, to achieve the best results. We utilized the PASCAL challenge dataset and addressed the class imbalance problem by aggregating diseases in one instance and employing appropriate metrics in another.

Several studies have explored heart disease prediction using machine learning. Zhang et al. [12] utilized a Support Vector Machine (SVM) model with spectrogram features, achieving a precision of 0.76, while Deng et al. [6] used SVM with Discrete Wavelet Transform (DWT) features, obtaining similar precision. Although these models are computationally efficient, their performance is limited. Advancements in deep learning, such as the Long Short-Term Memory (LSTM) model used by Raza et al. [10] with 1D time series features, achieved an accuracy of 0.80 with Normal, Murmur, and Extrasystole classes.

Significant improvements in accuracy were achieved using Convolutional Neural Networks (CNNs) by Alafif et al. [2] and Noman et al. [9], although they only considered Normal and Abnormal classes. A more disease-specific approach was taken by Chen et al. [4], who used a 2D CNN model with Wavelet Transform and Hilbert-Huang features, achieving an accuracy of 0.93 with Normal, Murmur, and Extrasystole classes. This high accuracy high-

lights the potential for improving our support model, which struggles to distinguish between Murmur, Normal, and Extrasystole classes.

Direct comparisons between studies are challenging due to differences in datasets and class definitions. Our model uniquely considers five classes, making it distinct from others. Furthermore, the choice of evaluation metrics is crucial when dealing with imbalanced datasets, as accuracy can be misleading.

Our research contributes to the literature by presenting two models. MLP_Ensemble5 was optimized to minimize false normals while maintaining low computational costs and distinguishing between disease presence and artifact signals. MLP_Ensemble2 was optimized for overall performance and introduced explainability measures to assist medical staff.

Despite these advancements, our project faced limitations. The limited dataset size prevented the creation of a validation set, potentially biasing results. Additionally, to increase data availability, we selected a one-second extraction interval, which may not be optimal due to varying heart rates. This approach might result in samples lacking relevant information if the full cardiac cycle is not present within the interval.

Feature selection also posed challenges. While MFCCs proved effective, they were not sufficiently discriminative for distinguishing between Normal, Murmur, and Extrasystole classes, where our model struggled the most. Furthermore, the explainability of the model has its constraints. We identified significant temporal regions on the waveform based on MFCC values within these regions. According to SHAP values, these specific MFCC values help to classify the sample correctly. However, the model only understands the average temporal values, not the instantaneous ones. Consequently, the explanation provided by the model is limited and requires further validation to be considered reliable.

Finally, the representativeness of the dataset remains a major obstacle to developing a model suitable for real-world scenarios. Addressing these limitations in future research could enhance the applicability and reliability of our models in clinical settings.

5. CONCLUSION

In this project, we have developed a machine learning model aimed at improving heart disease detection. Utilizing advanced ensemble techniques, we optimized two models : MLP_Ensemble5 and MLP_Ensemble2. The MLP_Ensemble5 model was specifically fine-tuned to minimize false normals while maintaining low computational costs. On the other hand, MLP_Ensemble2 focused on overall performance and incorporated explainability measures to aid medical professionals in decision-making.

Despite the notable advancements, our project faced several limitations. The size of the dataset constrained our ability to create a validation set, which might have introduced biases in the results. Additionally, the one-second extraction interval used to increase data availability could

have resulted in missing critical information from complete cardiac cycles. Feature selection posed another challenge, as Mel Frequency Cepstral Coefficients (MFCCs), while effective, were not sufficiently discriminative for certain heart conditions like Murmur and Extrasystole.

Moreover, the model's explainability, while a significant feature, had limitations. The reliance on average temporal values rather than instantaneous ones meant that the explanations provided by the model were not always fully reliable and required further validation.

5.1. Future Works

Future research should address the limitations identified in this project to enhance the model's applicability and reliability in real-world clinical settings. Specifically, expanding the dataset and improving its representativeness will be crucial. A larger and more diverse dataset will capture a wider range of heart sound variations, improving the model's ability to generalize across different patient populations and conditions. Collaborating with multiple healthcare institutions to collect more comprehensive data, which includes diverse demographic and clinical characteristics, will be essential.

Optimizing the extraction intervals to capture complete cardiac cycles could lead to better model performance. The current one-second intervals may miss critical information. By adjusting extraction intervals to encompass entire cardiac cycles, the model will analyze more comprehensive heartbeat patterns, enhancing its accuracy in detecting subtle abnormalities.

Exploring alternative feature extraction techniques is another important area. While MFCCs have been effective, they may not capture all relevant features of heart sounds. Methods such as wavelet transforms or more complex neural features derived from deep learning models, such as CNNs or RNNs, could also be explored to enhance feature extraction and model performance.

Finally, enhancing the model's explainability will be essential for its clinical adoption. Collaborating with medical professionals to analyze the results of the explainability procedure will ensure the medical relevance of the identified waveform zones.

6. APPENDIX

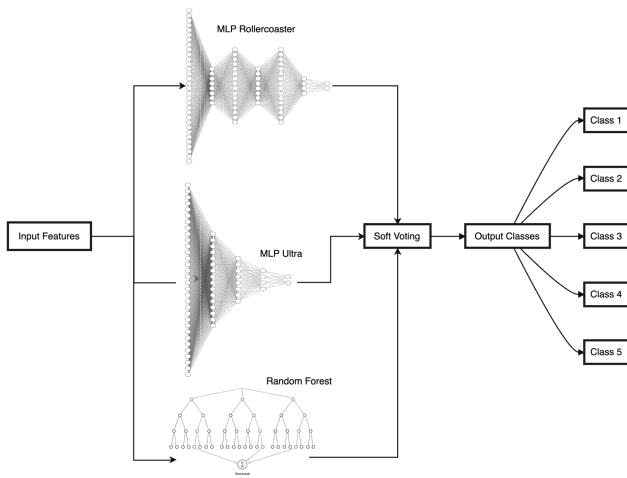


Fig. 25: MLP Ensemble5 Architecture

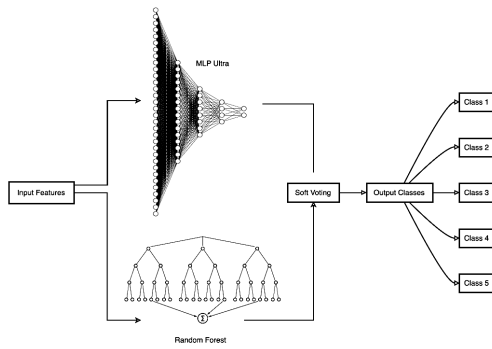


Fig. 26: Architecture of the best Support Model

REFERENCES

- [1] en. URL: <https://www.kaggle.com/datasets/mersico/dangerous-heartbeat-dataset-dhd>.
- [2] Tarik Alafif et al. "Normal and Abnormal Heart Rates Recognition Using Transfer Learning". In: *2020 12th International Conference on Knowledge and Systems Engineering (KSE)*. Nov. 2020, pp. 275–280. DOI: [10.1109/KSE50997.2020.9287514](https://doi.org/10.1109/KSE50997.2020.9287514). URL: <https://ieeexplore.ieee.org/abstract/document/9287514>.
- [3] P. Bentley et al. *The PASCAL Classifying Heart Sounds Challenge 2011 (CHSC2011) Results*. URL: <http://www.peterjbentley.com/heartchallenge/index.html>.
- [4] Lili Chen et al. "The Diagnosis for the Extrasystole Heart Sound Signals Based on the Deep Learning". In: *Journal of Medical Imaging and Health Informatics* 8.5 (June 2018), pp. 959–968. DOI: [10.1166/jmihi.2018.2394](https://doi.org/10.1166/jmihi.2018.2394).
- [5] Wei Chen et al. "Deep Learning Methods for Heart Sounds Classification: A Systematic Review". In: *Entropy* 23.6 (May 2021), p. 667. ISSN: 1099-4300. DOI: [10.3390/e23060667](https://doi.org/10.3390/e23060667).
- [6] Shi-Wen Deng and Ji-Qing Han. "Towards heart sound classification without segmentation via autocorrelation feature and diffusion maps". In: *Future Generation Computer Systems* 60 (July 2016), pp. 13–21. ISSN: 0167-739X. DOI: [10.1016/j.future.2016.01.010](https://doi.org/10.1016/j.future.2016.01.010).
- [7] Aaron Fisher, Cynthia Rudin, and Francesca Dominici. *All Models are Wrong, but Many are Useful: Learning a Variable's Importance by Studying an Entire Class of Prediction Models Simultaneously*. 2019. arXiv: [1801.01489](https://arxiv.org/abs/1801.01489) [stat.ME]. URL: <https://arxiv.org/abs/1801.01489>.
- [8] Scott M. Lundberg and Su-In Lee. "A unified approach to interpreting model predictions". In: *CoRR* abs/1705.07874 (2017). arXiv: [1705.07874](https://arxiv.org/abs/1705.07874). URL: <http://arxiv.org/abs/1705.07874>.
- [9] Fuad Noman et al. "Short-segment Heart Sound Classification Using an Ensemble of Deep Convolutional Neural Networks". In: *ICASSP 2019 - 2019 IEEE International Conference on Acoustics, Speech and Signal Processing (ICASSP)*. May 2019, pp. 1318–1322. DOI: [10.1109/ICASSP.2019.8682668](https://doi.org/10.1109/ICASSP.2019.8682668). URL: <https://ieeexplore.ieee.org/abstract/document/8682668>.
- [10] Ali Raza et al. "Heartbeat Sound Signal Classification Using Deep Learning". en. In: *Sensors* 19.2121 (Jan. 2019), p. 4819. ISSN: 1424-8220. DOI: [10.3390/s19214819](https://doi.org/10.3390/s19214819).
- [11] Max Roser. "Causes of death globally: what do people die from?" In: *Our World in Data* (2021). <https://ourworldindata.org/causes-of-death-treemap>.
- [12] Wenjie Zhang, Jiqing Han, and Shiwen Deng. "Heart sound classification based on scaled spectrogram and tensor decomposition". In: *Expert Systems with Applications* 84 (Oct. 2017), pp. 220–231. ISSN: 0957-4174. DOI: [10.1016/j.eswa.2017.05.014](https://doi.org/10.1016/j.eswa.2017.05.014).